
**Separation Science and Technology**
Publication details, including instructions for authors and subscription information:
http://www.informaworld.com/smpp/title~content=t713708471

# Non-dispersive Solvent Extraction of Alkali Metals with the Dicyclohexano 18 Crown 6: Evaluation of Mass Transfer Coefficients

Jaouad Haddaoui[a]; Dominique Trébouet[a]; José Miguel Loureiro[b]; Michel Burgard[a]
[a] Laboratoire des Procédés de Séparation, UMR, CNRS 7512 ECPM, Strasbourg, Cedex 2, France [b] Laboratory of Separation and Reaction Engineering, Universidade do Porto, Faculdade de Engenharia, Porto, Portugal

Online publication date: 08 July 2010

**To cite this Article** Haddaoui, Jaouad , Trébouet, Dominique , Loureiro, José Miguel and Burgard, Michel(2004) 'Non-dispersive Solvent Extraction of Alkali Metals with the Dicyclohexano 18 Crown 6: Evaluation of Mass Transfer Coefficients', Separation Science and Technology, 39: 16, 3839 — 3858
**To link to this Article: DOI:** 10.1081/SS-200043001
**URL:** http://dx.doi.org/10.1081/SS-200043001

SEPARATION SCIENCE AND TECHNOLOGY
Vol. 39, No. 16, pp. 3839–3858, 2004

# Non-dispersive Solvent Extraction of Alkali Metals with the Dicyclohexano 18 Crown 6: Evaluation of Mass Transfer Coefficients

**Jaouad Haddaoui,[1] Dominique Trébouet,[1,*] José Miguel Loureiro,[2] and Michel Burgard[1]**

[1]Laboratoire des Procédés de Séparation, ECPM, Strasbourg, France
[2]Laboratory of Separation and Reaction Engineering, Universidade do Porto, Faculdade de Engenharia, Porto, Portugal



## ABSTRACT

The aim of this study is both to check the feasibility of the membrane contactor for the extraction of alkali metals with the dicyclohexano 18 crown 6 as extractant and to obtain informations about the mass transfer of these metals. The influence of tube and shell side hydrodynamics on extraction rates is studied. High aqueous flow rates flowing inside the tubes increase extraction efficiency, on the other hand the organic diffusion layer seems to have a less important role on the mass transfer. Initial extraction rate order follows the order of the extraction equilibrium. The mass transfer coefficients of alkali cation are calculated by performing an unsteady

*Correspondence: Dominique Trébouet, Laboratoire des Procédés de Séparation, UMR, CNRS 7512 ECPM, 25 rue Becquerel, 67087, Strasbourg, Cedex 2, France; E-mail: trebouetd@ecpm.u-strasbg.fr.



DOI: 10.1081/SS-200043001 0149-6395 (Print); 1520-5754 (Online)

state material balance and compared with values calculated by the resistance in series model and by a steady state model.

*Key Words:* Membrane contactor; Non-dispersive solvent extraction; Mass transfer calculation; Macrocycle extractant; Crown ether.



## INTRODUCTION

The membrane-based solvent extraction, also called pertraction, is shown as an alternative to the conventional extraction in mixer-settlers and counter current columns. Membrane-based solvent extraction is characterized by the immobilization of the aqueous–organic interface in the membrane pores. One of the two fluids wets the membrane by filling in pores. To prevent the mixing that would occur, slight overpressure must be applied to the other phase in order to stabilize the interface at the pore mouth. This microporous membrane offers several advantages over conventional extractors. The known and constant interfacial area in this type of contactors interfacial allows easier predictions than with conventional dispersed phase contactors. The use of a hollow fiber membrane module provides a large contact area per unit equipment volume by the use of compact device (20–100 times more surface area per volume). Moreover, no density difference between both fluids is required and emulsion formation is avoided because of the absence fluid/fluid dispersion. In our approach, the membrane is considered merely as a physical support for the liquid–liquid interface which increases the resistance to mass transfer. The membrane contactors are increasingly being used in a variety of fields including fermentation, pharmaceutical applications, chiral separation, and extraction of various pollutants from wastewaters, protein extraction and metal ion extraction use.[1] The feasibility of hollow fiber membrane contactors for processing radioactive wastes has received a growing attention in recent years. The particular treatment of long-lived radionuclides (actinides, iode, and cesium) needs a good extraction performance. Several examples of actinides extraction using membrane contactors have been reported. Kathios et al.[2] described the use of membrane contactor for the extraction of neodymium with DHDECMP (dihexyl-*N*,*N*-diethylcarbamoylmethyl-phosphonate) and CMPO (*n*-octyl(phenyl)-*N*,*N* diisobutylcarbamoylmethylphosphine oxide). Neodymium was chosen because this element is not radioactive but behaves similarly to trivalent americium, a long-lived actinide. Aqueous and organic phases flowed on the tube and shell side, respectively, in counter current mode. High organic and low aqueous flow rates gave best results for the extraction. The low flow rate of the feed stream provided a long contact time between both phases and increased the

mass transfer. While the high flow rate of the extracting fluid maintained the maximum driving force by keeping the solute concentration low. Regarding the difficult selective extraction of trivalent actinides over fission lanthanides from acidic media, Geist et al.[3] used a synergistic mixture of *bis*(chlorophenyl)dithiophosphinic acid and tri-*n*-octyl phosphine oxide in tert-butyl benzene in hollow fiber module for americium(III)–lanthanide separation. Up to 99,99% americium could be extracted from 0.5 kmol $m^{-3}$ nitric acid, with approximately one third of the lanthanides being co-extracted. They demonstrated the influence of operating mode on extraction efficiency.

The selective extraction of alkali metals and alkaline earths by macrocycles as crown ether and calix[4]arene has been investigated extensively by our group with among others the use of liquid membrane. These studies have shown that the complexation reaction of alkali metal with crown ether is fast as compared to the diffusion. The mass transfer is controlled by diffusion.[4,5] These macrocycles can recognize a metal ion by the size of their cavity. Therefore, macrocycles and hollow fiber module combination seems to be an attractive process, combining selectivity, and efficiency.[6]

This study is a preliminary evaluation of microporous hollow fiber membrane modules for the liquid–liquid extraction of alkali metal by macrocycle in chloroform. So, a crown ether is first used to optimize the operating conditions. This expertise will then be applied to extraction by calix[4]arene and the use of more conventional diluents (aromatic hydrocarbons) will also be investigated. The aim of this study is to check the feasibility of the non-dispersive solvent extraction and to obtain useful informations about the mass transfer of alkali metals with the dicyclohexano 18 crown 6 as extractant. In order to improve the understanding of mass transfer in membrane contactors and to identify the controlling step, the influences of operating mode on extraction efficiency, tube side and shell side hydrodynamics were studied. Various models are developed in the literature.[7–10] In the present paper, the extraction of alkali cations with DC 18-6 is described by performing an unsteady-state mass balance on the module and considering a rapid extraction reaction. Comparisons with a steady state model developed by D'Elia[9] and the common resistance in series model[1] are made.

## MATERIAL AND METHODS

### Reagents and Solutions

The organic solution was prepared by dissolving dicyclohexano 18 crown 6 (abbreviate as DC 18-6) in chloroform (Prolabo, RP Normapur, >99% purity). The different aqueous phases were prepared by dissolving $KNO_3$

(Fluka, >99.5% purity), $RbNO_3$ (Fluka, >99% purity), and $CsNO_3$ (Aldrich, >99.9% purity) in deionized water.

## Partition Coefficients between Water and DC18-6 in Chloroform

In order to determine extraction equilibrium isotherms, 5 mL of an aqueous solution of each alkali cation ($K^+$, $Rb^+$, and $Cs^+$), at different concentration (from $1 \times 10^{-4}$ to $5 \times 10^{-3}$ M) were added with equal volumes (5 mL) of DC18-6 chloroform solutions. The total concentration of DC18-6 is always $1 \times 10^{-3}$ M. Ionic strength is maintained constant by adding $LiNO_3$ (0.2 M). The total volume of the sample was placed in screw capped flasks and mechanically mixed and thermostated in a water bath at 25°C. It was verified that the system studied here had reached equilibrium after a 45 min period. Once the two phases had settled, they were separated by centrifugation. The concentration of alkali cations was determined in both phases.



## Membrane Type and Module

The module contains 300 hollow fiber polypropylene fibers Celgard X-10 (Hoechst Celanese, Germany). The characteristics of the module and fiber are described in Table 1.

## Membrane Contactor Experiments

The aqueous solution flowed through the fiber lumen whereas the solvent stream flowed through the shell space. Prior to experiments, the pure organic phase (chloroform) and pure water were fed, respectively, into the inner side and in the shell so as to condition hollow fibers. Owing to the hydrophobic nature of the fibers, a slight pressure (0.2 bar) was applied to the aqueous phase in order to stabilize the interface within the membrane and ensuring that no displacement of the organic phase and emulsion formation took place. All the experiments were carried out at constant temperature, 25°C, using feed jacketed glass beakers for both the aqueous and organic phases. The aqueous phase and solvent phase reservoirs were 200 and 100 mL, respectively. The extraction rate is increased and the ionic strength is maintained constant by adding lithium nitrate (0.2 M) in aqueous phase. The tube side flow velocity, $u_w$, ranged from 2.5 to 12.3 cm $sec^{-1}$ and the shell side flow velocity, $u_s$, ranged from 0.4 to 1.5 cm $sec^{-1}$. With the

***Table 1.*** Characteristics of hollow fibers module and membrane Celgard X-10.

| | |
|---|---|
| Module | |
| Material | Polypropylene |
| Number of fibers | 300 |
| Length | 35 cm |
| Fiber length | 25.4 cm |
| Diameter | 1.2 cm |
| Exchange area | 0.017 $m^2$ |
| Exchange specific area | 6 $m^{-1}$ |
| Membrane fiber Celgard X-10 | |
| Material | Polypropylene |
| Internal diameter[a] | 240 μm |
| Wall thickness[a] | 30 μm |
| Porosity, $\varepsilon$[a] | 30% |
| Tortuosity (estimated), $\tau$[b] | 3.33 |
| Pore size[a] | 0.05 μm |

[a]From Hoescht Celanese catalogue and Peretti et al.[11]
[b]The tortuosity can be expressed by the Wakao-Smith relation.[12]



system studied here, the concentration change during a single pass is negligible owing to the small interfacial area and to the low distribution coefficient. In order to increase the change in concentration, extraction is carried out with recirculation of the feed and organic phases through the module and back into the feed and organic reservoirs, respectively, and both streams were recirculated to reservoirs, so the measured concentration asymptotically reached an equilibrium value. Both phases were regularly sampled and analyzed: 1 mL for the aqueous phase and 2 mL for the organic phase. This volume variation was considered in the mass balance. The experiments were designed to analyze the influence of both aqueous and organic flow rates on the overall mass transfer coefficient. The system set up is shown in Fig. 1.

## Analytical Method

The concentrations of alkali cations in aqueous phase were directly measured by atomic absorption (Perkin Elmer). The alkali cation analysis in organic phase by atomic absorption require a stripping step: 5 mL of organic phase was shaken with an equal volume of ultra pure aqueous phase for 2 hr.

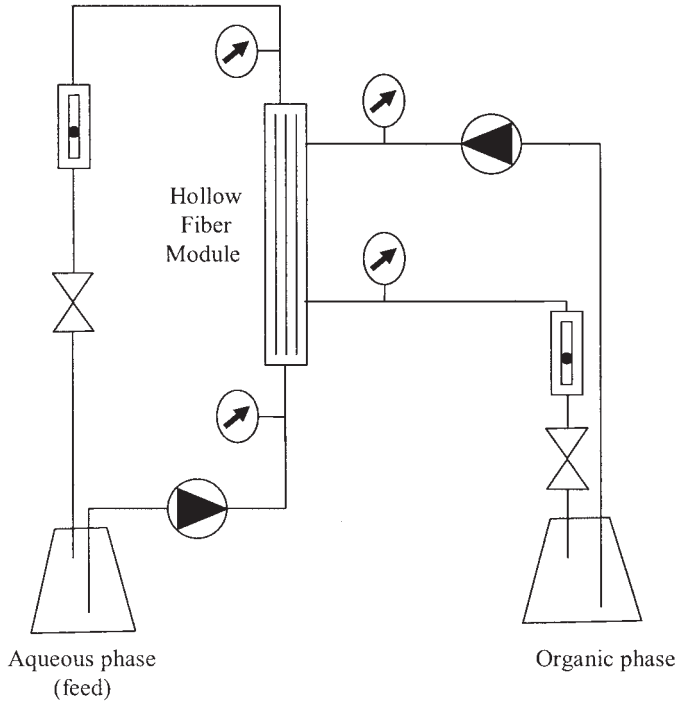


***Figure 1.*** Experimental setup for the extraction of alkali metals.



## EXTRACTION EQUILIBRIUM

Before the membrane contactor experiments were carried out, equilibrium conditions had to be determined as a basic study for mass transfer coefficient calculations. On the basis of previous studies,[4,13] it can be considered that the overall extraction equilibrium of alkali nitrates ($KNO_3$, $RbNO_3$, and $CsNO_3$) with an electroneutral ligand (DC 18-6, called L) can be expressed as follows:

$$\bar{L} + NO_3^- + M^+ \leftrightarrows \overline{MLNO_3} \tag{1}$$

where the overbar refers to the organic phase and $M^+$ to the alkali metal. The dissociation of $\overline{MLNO_3}$ into $NO_3^-$ and $ML^+$ in the organic phase and the association between $M^+$ and $NO_3^-$ in the aqueous phase are neglected because the value of chloroform dielectric constant is low (4.8) and the

value of water dielectric constant is high.[13] The partition coefficient $P$ and the equilibrium constant ($K_E$) of Eq. (1) are given by:

$$P = \frac{(\overline{MLNO_3})}{(M^+)} \tag{2}$$

$$K_E = \frac{(\overline{MLNO_3})}{(M^+)(\bar{L})(NO_3^-)} \tag{3}$$

The equilibrium solvent phase concentration as a function of the equilibrium aqueous phase concentration is shown for each metal in Fig. 2. Values which are shown in Table 2 are relatively low. In the literature, the previous studies on membrane contactors cover a wide range of partition coefficients from about $1 \times 10^{-1}$ to $1 \times 10^{3}$ M.[14] Table 2 presents the extraction equilibrium constant $K_E$ and the corresponding extraction yields ($E\%$). The extraction of three alkali cations by the crown ether DC 18-6 is low and similar. These results can be notably explained by the low solubility of $NO_3^-$ in a low polar diluent (chloroform). It is very slightly higher for the potassium than for rubidium and cesium, according to the well-known cavity size selectivity concept.[15] On the basis of a previous study[4] and from partition coefficient expression, a model has been developed to predict

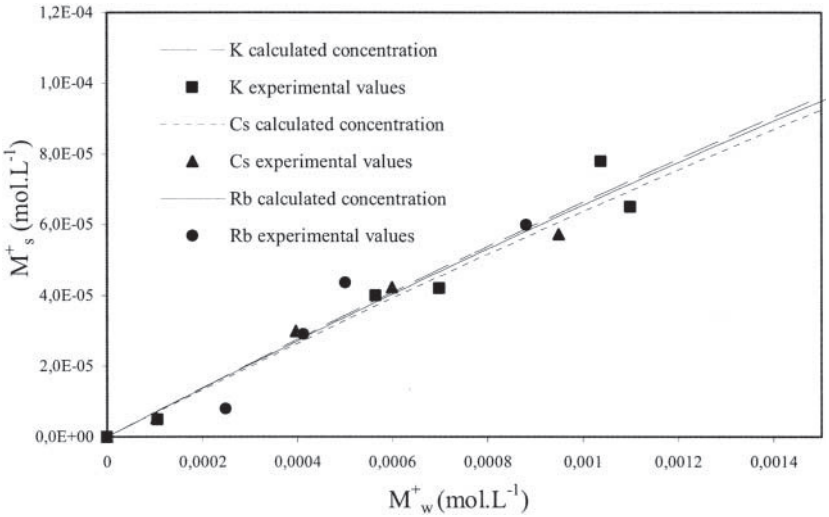


***Figure 2.*** Equilibrium curves of alkali nitrates partitioning between water and DC18-6 ($1 \times 10^{-3}$ M) in chloroform at 25°C. (■, ●, ▲) experimental data and (—) model prediction. ($LiNO_3 = 0.2$ M).

***Table 2.*** Partition coefficients, extraction yields, and equilibrium constants at 25°C.

| | $K^+$ | $Rb^+$ | $Cs^+$ |
|---|---|---|---|
| $P^a$ | 0.076 | 0.072 | 0.061 |
| $E$ (%)[a] | 6.8 | 6.4 | 5.3 |
| Log $K_E$ | 2.60 | 2.56 | 2.51 |

[a]Calculated for (DC18-6) $= 1 \times 10^{-3}$ M and $(M^+)_{aq} = 1 \times 10^{-3}$ M, $(LiNO_3) = 0.2$ M.

the equilibrium relationship. The following Eq. (4) gives the relation between the concentration of the metal in the aqueous phase and the organic phase:

$$C_s = \frac{C_w \cdot K_E \cdot (L_o) \cdot (NO_3^-)}{1 + C_w \cdot K_E \cdot (NO_3^-)} \tag{4}$$

where $C_s$ and $C_w$ represent, respectively, the equilibrium concentrations of solute in the organic and aqueous phases, $(L_o)$ the initial concentration of crown ether in aqueous phase. $K_E$ is the extraction constant of alkali nitrates by DC18-6.

The equilibrium curves in the concentration range of this study (the membrane contactor experiments are carried out with a metal initial concentration of about $1 \times 10^{-3}$ mol $L^{-1}$) show that the partition coefficients do not vary significantly during the extraction process and can be considered as constant (linear isotherms). From Eqs. (2) and (3), the coefficient partition can be written as $P = K_E \cdot (L_o) \cdot (NO_3^-)$ as far as the ligand initial concentration $(L_o)$ is much higher than the metal cation concentration in organic phase and will be used in transfer treatment below.

## LIQUID–LIQUID EXTRACTION IN HOLLOW FIBERS MODULE

### Effect of Aqueous and Organic Flow Rates on Mass Transfer Kinetics

The use of low concentration of alkali metals and the back extraction needed to analyze these elements present in the organic phase could lead to possible losses. Many precautions were taken to minimize experimental errors. Mass balances that are stated as a control for the quality of the

experiments were systematically checked after extraction experiments. Mass balances were about 98% for the different alkali metals. The flow rates of both phases were alternately modified, with all the other parameters kept constant. Figure 3 shows potassium extraction kinetic curves obtained for different aqueous and organic phase flow rates. The aqueous flow rate had a more significant influence on the extraction rate than the organic flow rate. Similar results are observed for the cesium and for the rubidium. With a tube-side flow velocity of 12.3 cm sec$^{-1}$, the extraction yields obtained in 90 min are overall in agreement with values obtained in static conditions: from 6% for the potassium to 5% for the cesium. The diffusion of alkali metal from the bulk aqueous phase to the aqueous–organic interface, through the aqueous boundary layer seems to be the limiting step. The organic diffusion layer seems to have a less important role on the mass transfer although the low partition coefficient values which indicate that the solute has a higher affinity for the aqueous phase[14] and the diffusivities of the metal complex ($\overline{MLNO_3}$) in organic phase are lower than the diffusivity of metal ion in aqueous phase (Table 3). The values of diffusivity, $D$ for the complex DC18 C6–alkali cation in chloroform are estimated by the Wilke-Chang equation. The molar volume of crown ether at its normal boiling point is 362 cm$^3$ mol$^{-1}$ calculated by the method of additive group contribution.[17,18] The alkali cation is inside the crown ether cavity, so we assume that the diffusion of complex is close to the diffusion of the crown ether. This surprising increase of alkali cation flux

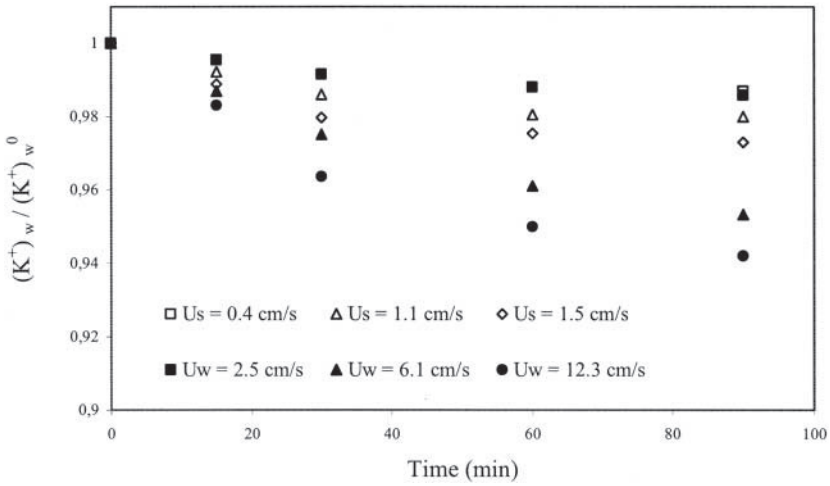


***Figure 3.*** Effect of aqueous and organic flow rate on potassium extraction kinetics (▲, ■, ◆: $u_s = 0.4$ cm sec$^{-1}$ and □, ◇, △: $u_w = 2.5$ cm sec$^{-1}$).

***Table 3.*** Values of parameters used for resistance in series model.

| Parameter | $K^+$ | $Rb^+$ | $Cs^+$ | Reference |
|---|---|---|---|---|
| Diffusivity ($m^2\,sec^{-1}$) | | | | |
| $D_{M,w}$ | $1.96 \times 10^{-9}$ | $2.07 \times 10^{-9}$ | $2.06 \times 10^{-9}$ | [16] |
| $D_{NO_3},w$ | $1.90 \times 10^{-9}$ | $1.90 \times 10^{-9}$ | $1.90 \times 10^{-9}$ | [16] |
| $D_{MNO_3},w$ | $1.93 \times 10^{-9}$ | $1.98 \times 10^{-9}$ | $1.97 \times 10^{-9}$ | [16] |
| $D_{MLNO_3},s$ | $1.29 \times 10^{-9}$ | $1.29 \times 10^{-9}$ | $1.29 \times 10^{-9}$ | [17,18] |
| Mass transfer coefficient ($m\,sec^{-1}$) | | | | |
| $k_m$ | $2.2 \times 10^{-6}$ | $2.2 \times 10^{-6}$ | $2.2 \times 10^{-6}$ | This work |

with increasing aqueous phase flow velocity may be explained by the module configuration. The flow area is lower inside the hollow fibers ($540\,cm^2$) than in the shell side ($760\,cm^2$) and induces a pressure drop more important in the aqueous phase side.[19] This overpressure ($\sim 0.2$ bar) causes a moving of interface from inside (aqueous side) to outside (organic side) of pores leading to a reduction of organic layer thickness in pores. High aqueous flow velocities ($>15\,cm\,sec^{-1}$) for a constant organic flow velocity lead to a dispersion of aqueous phase in the organic phase.

## Evaluation of Mass Transfer Coefficients

The mass transfer process is described in literature as successive steps.[1,20] The metal ions diffuse through the aqueous layer to the aqueous–membrane interface. The metal complex formed at this interface diffuses across organic solution in the microporous wall into the organic solution on the outer side of the fibers. Previous studies concerning the alkali metal transfer across a liquid membrane have shown that the complexation reaction of the alkali metal with crown ether is fast as compared to the diffusion. The mass transfer is controlled by diffusion.[4,5,21] The description of the mass transfer for the solute is based on the setting and solving of appropriate mass balance equations for an unsteady state inside the module fibers (aqueous phase):

$$Q_w \frac{\partial C_w}{\partial z} + \frac{4V_m}{d_{in}L} K_w \left( C_w - \frac{C_s}{P} \right) + \frac{V_m}{L} \frac{\partial C_w}{\partial t} = 0 \tag{5}$$

and on the module fibers shell side (organic phase):

$$Q_s \frac{\partial C_s}{\partial z} + \frac{4V_m}{d_{in}L} K_w \left( C_w - \frac{C_s}{P} \right) - \frac{V_c}{L} \frac{\partial C_s}{\partial t} = 0 \tag{6}$$

$C_w$ and $C_s$ are, respectively, the concentration of alkali metal in aqueous phase and in organic phase, $Q_w$ and $Q_s$ are, respectively, the aqueous phase and organic phase flowrates. $V_m$ is the volume of the aqueous phase inside the hollow fiber and is defined by the following equation:

$$V_m = N_f \pi \frac{d_{in}^2}{4} L \tag{7}$$

$V_c$ is the volume of organic phase inside the module (total internal volume of the module minus volume occupied by the fibers). $L$ is the length of hollow fiber, $N_f$ is the number of fibers and $d_{in}$ is the internal diameter of hollow fiber. $K_w$ represents the overall mass transfer coefficient from aqueous phase to organic phase. The convention that the aqueous phase always flows from $z = 0$ (entry of aqueous phase) to $z = L$ (entry of organic phase) is adopted. The boundary conditions for this system, Eqs. (5) and (6), are:

$$t = 0 \qquad 0 < z < L \qquad C_w = C_w^0 \quad \text{and} \quad C_s = 0 \tag{8}$$

$$\begin{aligned} t > 0 \qquad & z = 0 \qquad && C_w = C_{w0} \\ & z = L \qquad && C_s = C_{sL} \end{aligned} \tag{9}$$

The concentrations at the module inlet ($C_{w0}$ and $C_{sL}$, respectively) are given by the material balances applied to the corresponding reservoirs:

Reservoir containing the aqueous phase:

$$Q_w C_{wL} = Q_w C_{w0} + V_w \frac{dC_{w0}}{dt} \tag{10}$$

Reservoir containing the organic phase:

$$Q_s C_{s0} = Q_s C_{sL} + V_s \frac{dC_{sL}}{dt} \tag{11}$$

with the following initial conditions:

$$t = 0 \quad C_{w0} = C_w^o \quad \text{and} \quad C_{sL} = C_s^o = 0 \tag{12}$$

Introducing dimensionless variables:

$$x = \frac{z}{L}; \quad f_w = \frac{C_w}{C_w^o}; \quad f_s = \frac{C_s}{PC_w^o}; \quad \theta = \frac{t}{\tau_{wm}} \quad \text{with} \quad \tau_{wm} = \frac{V_m}{Q_w} \tag{13}$$

the model Eq. (5), (6), (10), and (11) can be written in dimensionless form:

$$\frac{\partial f_w}{\partial \theta} + \frac{\partial f_w}{\partial x} + N_d(f_w - f_s) = 0 \tag{14}$$

$$\frac{\partial f_s}{\partial \theta} - \frac{\tau_{wm}}{\tau_{sc}} \frac{\partial f_s}{\partial x} - \frac{N_d}{\xi}(f_w - f_s) = 0 \tag{15}$$

$$\frac{df_{w0}}{d\theta} = \frac{\tau_{wm}}{\tau_{ww}}(f_{wL} - f_{w0}) = \frac{V_m}{V_w}(f_{wL} - f_{w0}) \tag{16}$$

$$\frac{df_{sL}}{d\theta} = \frac{\tau_{wm}}{\tau_{ss}}(f_{s0} - f_{sL}) = \frac{V_c}{V_s} \cdot \frac{\tau_{wm}}{\tau_{sc}}(f_{s0} - f_{sL}) \tag{17}$$

In the foregoing equations, four space times (two for each phase, for the module and the reservoir, respectively) were introduced. Their definitions are:

$$\tau_{wm} = \frac{V_m}{Q_w}; \quad \tau_{sc} = \frac{V_c}{Q_s}; \quad \tau_{ww} = \frac{V_w}{Q_w} \quad \text{and} \quad \tau_{ss} = \frac{V_s}{Q_s} \tag{18}$$

Moreover, one equilibrium (the capacity factor $\xi$) and one mass transfer (the number of mass transfer units $N_d$) dimensionless parameters were also introduced. Their definitions are, respectively:

$$\xi = \frac{PV_c}{V_m} \quad \text{and} \quad N_d = \frac{\tau_{wm}}{\tau_d} \quad \text{with} \quad \tau_d = \frac{d_{in}}{4K_w}$$

(time constant for mass transfer)

Five dimensionless parameters control the behavior of the system, namely the aforementioned equilibrium ($\xi$) and mass transfer ($N_d$) parameters, one ratio of space times ($\tau_{wm}/\tau_{sc}$) and two volume ratios ($V_m/V_w$ and $V_c/V_s$).

The dynamic response of the system is determined by simultaneously solving the system of coupled partial differential equations (14) and (15) and ordinary differential equations (16) and (17) with a FORTRAN program using the software package PDECOL[22] using the Equilibrium data (Table 2) together with the operating data given in Table 4. In Fig. 4, the experimental and adjusted calculated aqueous phase concentrations vs. time are shown for the three alkali metals and for given aqueous and organic phase velocities. The adjustment is carried out by varying the overall mass transfer coefficients, $K_w$. The values of overall mass transfer coefficients for the three alkali metals and for different aqueous and organic phase velocities are presented in Table 5. The overall mass transfer coefficient increases mainly with the aqueous phase flow velocity.

D'Elia et al.[9] proposed a simplified mathematical treatment of mass balance by assuming a steady state regime. In this closed system, approximation is valid if reservoir concentrations change slowly with time. This is realized if the volume of the reservoirs are much larger than the volume of the module. The combination and integration of mass balance equations

***Table 4.*** Operating data used to solve the system of differential equations.

| Parameter | Value |
|---|---|
| Initial concentrations of alkali metal in aqueous phase | $1.10^{-3}$ M |
| Initial concentrations of alkali metal in organic phase | 0 M |
| Volumetric flow rate of aqueous phase | $3.3 \times 10^{-7}$ to $1.7 \times 10^{-6}$ m$^3$ sec$^{-1}$ |
| Volumetric flow rate of organic phase | $3.3 \times 10^{-7}$ to $1.2 \times 10^{-6}$ m$^3$ sec$^{-1}$ |
| Hollow fibers tube overall volume | $3.44 \times 10^{-6}$ m$^3$ |
| Shell side volume | $1.91 \times 10^{-5}$ m$^3$ |
| Aqueous reservoir volume | $200 \times 10^{-6}$ m$^3$ |
| Organic reservoir volume | $100 \times 10^{-6}$ m$^3$ |



lead to Eq. (19) from which the overall mass transfer coefficients are deduced by plotting ln $(\Delta C_0/\Delta C)$ in the aqueous phase vs. time.[9,14]

$$\left[\frac{B + C\exp A}{E}\right]\ln\left[\frac{\Delta C_0}{\Delta C}\right] = t(1 - \exp A) \tag{19}$$

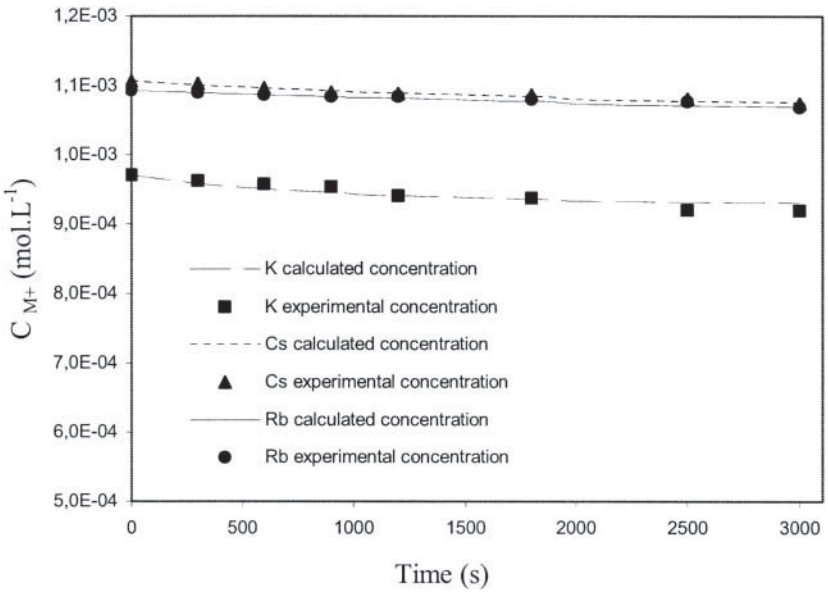


***Figure 4.*** Comparison between experimental and calculated concentrations for the three alkali metals ($u_w = 2.5\,\text{cm sec}^{-1}$ and $u_s = 0.4\,\text{cm sec}^{-1}$).

***Table 5.*** Mass transfer coefficients estimated by the unsteady model ($u_s = 0.4$ cm sec$^{-1}$).

| | $K_w$ (m sec$^{-1}$) | | |
|---|---|---|---|
| | $u_w = 2.5$ cm sec$^{-1}$ | $u_w = 6.1$ cm sec$^{-1}$ | $u_w = 12.3$ cm sec$^{-1}$ |
| Cs | $9.4 \times 10^{-10}$ | $1.5 \times 10^{-8}$ | $5.4 \times 10^{-8}$ |
| Rb | $5.5 \times 10^{-10}$ | $1 \times 10^{-8}$ | $4.5 \times 10^{-8}$ |
| K | $2.5 \times 10^{-9}$ | $6.5 \times 10^{-9}$ | $2.5 \times 10^{-8}$ |

where

$$\frac{\Delta C_0}{\Delta C} = \frac{C_w^o - (C_s^o/P)}{\left[C_w - \left(C_s^o/P\right)\right] - V_w/V_s P(C_w^o - C_w)} \tag{20}$$

$$A = -K_w S(B - C) \text{ with :} \tag{21}$$

$$B = \frac{1}{Q_w} \tag{22}$$

$$C = \frac{1}{PQ_s} \tag{23}$$

$$E = \frac{1}{V_w} + \frac{1}{PV_s} \tag{24}$$

Lastly, a third approach is considered which provides the overall mass transfer coefficient from the three individual or local mass transfer coefficients coming from:

- the feed aqueous phase (tube side), $k_w$
- the membrane, $k_m$
- the organic phase (shell side), $k_s$

In our case the aqueous phase flows inside the tube of a hydrophobic hollow fiber membrane, and the organic phase flows outside the tube so the resistance in series model relates the overall mass transfer coefficient $K_w$ to the local mass transfer coefficients by the following relation:[1]

$$\frac{1}{K_w} = \frac{1}{k_w} + \frac{d_{in}}{Pk_m d_{lm}} + \frac{d_{in}}{Pk_s d_{out}} \tag{25}$$

where $d_{in}$ and $d_{out}$ are the internal and external fiber diameters, respectively, and $d_{lm}$ their logarithmic mean value. The three terms in the right-hand side

of Eq. (25) are the resistances of aqueous layer diffusion ($R_{\text{aqueous}}$), membrane diffusion ($R_{\text{membrane}}$), and organic layer diffusion ($R_{\text{organic}}$).

Local mass transfer coefficients are predicted using various hydrodynamics patterns. The mass transfer coefficient $k_w$ for the tube side (aqueous phase) can be predicted with the Lévêque relation. The Lévêque relation is applicable to a laminar flow in a tube when the Graetz number is high ($Gz > 4$) and depends on the mean flow velocity $u_w$ according to Refs.[1,20]:

$$\frac{2r_{in}k_w}{D_{MNO_3}} = 1.62\left(\frac{4r_{in}^2 u_w}{D_{MNO_3}L}\right)^{1/3} \tag{26}$$

The Graetz number is defined by Eq. (27):

$$Gz = \frac{u_{tube}(d_{in})^2}{D_{MNO_3}\cdot L} \tag{27}$$

The mass transfer coefficient $k_m$ is evaluated by considering pure diffusion of the complex in the pores containing the organic phase (hydrophobic membrane) by using Fick's law in a cylindrical geometry:[20]

$$k_m = \frac{D_{MLNO_3}\varepsilon}{\tau r_{in}\ln(r_{out}/r_{in})} \tag{28}$$

The mass transfer coefficient $k_s$ is determined using a recent development[23] of the hydrodynamics in the shell side of hollow fiber modules taking into account the kinematic viscosity of the medium $\nu$, the fiber packing density within the module $\Phi$ which in our case equals 0.12 and the hydraulic radius of the shell $r_H$ which is calculated according to Lipnizki and Field:[24]

$$\frac{2r_H k_s}{D_{MLNO_3}} = 0.09(1-\Phi)\cdot\left(\frac{2r_H u_s}{\nu}\right)^{(0.8-0.16\Phi)}\left(\frac{\nu}{D_{MLNO_3}}\right)^{1/3} \tag{29}$$

The parameters used for the calculations and the membrane mass transfer coefficient calculated are listed in Table 3. In order to define the limiting step, the contribution of individual resistances to the overall resistance by using a relation of the type is used:

$$\%R_i = 100 \times \frac{R_i}{\sum_i R_i} \tag{30}$$

The contribution of the membrane resistance is approximately 90% and is consequently the main limiting step in the mass transfer. This major resistance does not depend on the hydrodynamic parameters. Moreover, the calculations

show that the contribution of the organic layer is 14.5% whereas the contribution of the aqueous layer is significantly lower (0.5%).

Figure 5 and Table 6 show the effect of the aqueous phase velocity on the overall mass transfer coefficient. The values obtained for the unsteady state model are to be considered as the most accurate. The global mass transfer coefficients calculated with this approach show the reduction of aqueous diffusion layer and organic layer inside pores.

The validity of the values obtained for the two other models clearly depend on the range of aqueous phase velocity. For low velocities the "steady state approximation" appears to be valid. According to Fig. 3, this is in agreement with the effect of the aqueous phase velocity on the evolution of the reservoir concentration. For low aqueous phase velocities, a pseudo steady state (weaker $\delta C/\delta t$) is quickly reached in the system. For higher aqueous flow rates, the concentration variation with time increases in the early step of the process and the steady state approximation becomes progressively less accurate.

It is also seen (Fig. 5 and Table 6) that resistance in series model provides mass coefficients which appear to be only weakly influenced by the aqueous phase velocity. This may be a consequence of the major membrane resistance contribution and highlights the difficulty to estimate the contribution of the aqueous phase layer to the overall mass transfer coefficient for low Graetz

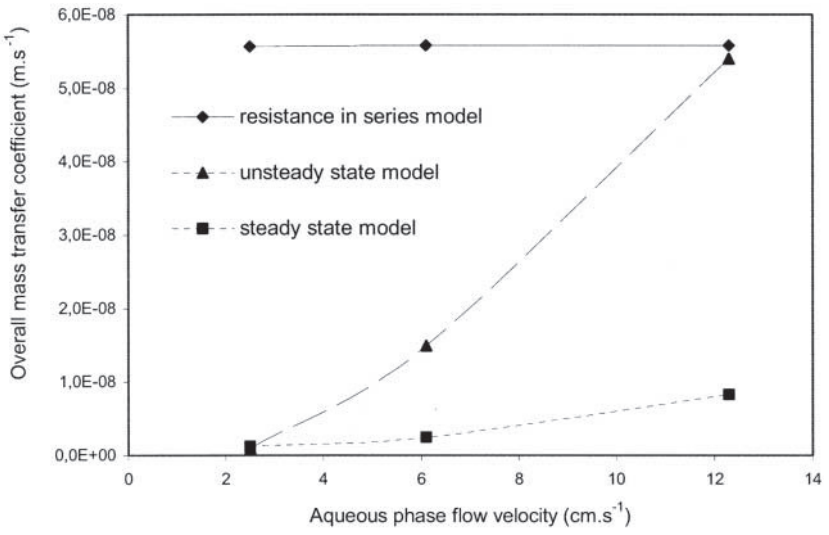


***Figure 5.*** Overall mass transfer coefficients of cesium vs. aqueous phase flow velocity ($u_s = 0.4\,\mathrm{cm\,sec^{-1}}$).

***Table 6.*** Comparison of calculated overall mass transfer coefficients.

| | $K_w$ (m sec$^{-1}$) ($u_w = 2.5$ cm sec$^{-1}$ and $u_s = 0.4$ cm sec$^{-1}$) | | |
|---|---|---|---|
| | Steady state model | Unsteady state model | Resistances-in-series model |
| Cs | $12 \times 10^{-10}$ | $9.4 \times 10^{-10}$ | $5.5 \times 10^{-8}$ |
| Rb | — | $5.5 \times 10^{-10}$ | $5.7 \times 10^{-8}$ |
| K | $1.9 \times 10^{-9}$ | $2.5 \times 10^{-9}$ | $6.9 \times 10^{-8}$ |

numbers which take values near 2 for the lowest velocities. In the case of high aqueous phase velocity ($>12.3$ cm sec$^{-1}$) where the calculated overall mass transfer coefficient by the resistance in series model and by the unsteady state model are close, the Graetz number is equal to 14. In the literature, Graetz numbers thresholds as different as 10,[14] 25,[25] 400[26] can be found.

Further studies are in progress in order to define the practical conditions which provide a more satisfactory evaluation of the aqueous phase contribution in our liquid–liquid extraction systems.

## CONCLUSION

In this paper, the viability of the application of non-dispersive solvent extraction to the alkali metals extraction using crown ether has been checked. The extraction rates obtained with membrane contactor are in agreement with values obtained in static conditions. The performance of the extraction may be improved using a diluent which will increase the solubility of nitrates. The use of calix[4]arene will also be considered.

The aqueous flow rate had a more significant influence on the extraction rate than the organic flow rate. The diffusion of alkali metal from the bulk aqueous phase to the aqueous–organic interface, through the aqueous boundary layer seems to be the limiting step. This surprising increase of alkali cation flux with increasing aqueous phase flow velocity may be explained by the module configuration. The unsteady state model predicted satisfactorily the experimental results. The mass transfer coefficient has been determined by comparison between experimental and simulated results. The following values have been obtained for aqueous phase and organic phase flow velocities of 2.5 and 0.4 cm sec$^{-1}$ respectively: $2.5 \times 10^{-9}$ m sec$^{-1}$ for the potassium, $5.5 \times 10^{-10}$ m sec$^{-1}$ for the rubidium and $9.4 \times 10^{-10}$ m sec$^{-1}$ for the cesium. The values of overall mass transfer coefficient obtained with the steady state and the unsteady state models seem to be coherent at low flow rate (2.5 cm sec$^{-1}$). A pseudo steady state is quickly reached in the system.

For higher aqueous flow rates, the steady state approximation becomes progressively less accurate whereas the resistance in series model seems to be better adapted.

## NOMENCLATURE

| | |
|---|---|
| $P$ | partition coefficient |
| $K_E$ | equilibrium constant |
| $Q$ | flow rate ($m^3\,sec^{-1}$) |
| $C$ | solute concentration($mol\,m^{-3}$) |
| $V$ | volume ($m^3$) |
| $V_m$ | volume of aqueous phase inside hollow fibers ($m^3$) |
| $V_c$ | volume of organic phase inside the module ($m^3$) |
| $L$ | length of the hollow fiber (m) |
| $N_f$ | number of fibers in the module |
| $t$ | time (sec) |
| $K$ | overall mass transfer coefficient ($m\,sec^{-1}$) |
| $k$ | local mass transfer coefficient ($m\,sec^{-1}$) |
| $d$ | diameter (m) |
| $r$ | radius (m) |
| $r_H$ | hydraulic radius of the shell (m) |
| $u$ | velocity ($m\,sec^{-1}$) |
| $D$ | diffusivity ($m^2\,sec^{-1}$) |
| $S$ | membrane area in the module ($m^2$) |

### Subscripts

| | |
|---|---|
| w | aqueous |
| s | organic |
| in | relative to the inside of the tubes |
| out | relative to the outside of the tubes |
| lm | logarithmic mean value |
| 0 and L | relative to the length of the tube |

### Superscripts

| | |
|---|---|
| 0 | relative to the initial time |

## REFERENCES

1. Gabelman, A.; Hwang, S.T. Hollow fiber membrane contactors. J. Membr. Sci. **1999**, *159*, 61–106.

2. Kathios, D.J.; Jarvinen, G.D.; Yarbro, S.L.; Smith, B.F. A preliminary evaluation of microporous hollow fiber membrane modules for the liquid–liquid extraction of actinides. J. Membr. Sci. **1994**, *97*, 251–261.
3. Geist, A.; Weigl, M.; Compper, K. Minor actinide partitioning by liquid–liquid extraction: using a synergistic mixture of *bis*(chlorophenyl)-dithiophosphonic acid and TOPO in a hollow fiber module for americium(II)–lanthanides(III) separation. Sep. Sci. Technol. **2002**, *37* (15), 3369–3390.
4. Delloye, T.; Burgard, M.; Leroy, J.F. Liquid–liquid extraction and transport through a water chloroform water liquid membrane of alkaline earth nitrates by dicyclohexano 18-crown-6. New J. Chem. **1989**, *13* (2), 139–144.
5. Yaftian, M.R. Propriétés extractantes et de transport d'une série de calix[4]arenas neuters fonctionnalisés par des groupements amide et phosphoryle vis à vis des cations métalliques. Université Louis Pasteur: Strasbourg, France, 1998; Ph.D. Thesis.
6. Kubota, F.; Kakoi, T.; Goto, M.; Furusaki, S.; Nakashio, F.; Hano, T. Permeation behaviour of rare earth metals with a calix[4]arene carboxyl derivative in a hollow-fiber membrane. J. Mem. Sci. **2000**, *165*, 149–158.
7. Daiminger, U.A.; Geist, A.G.; Nitsch, W.; Plucinski, P.K. Efficiency of hollow fiber modules for non dispersive chemical extraction. Ind. Eng. Chem. Res. **1996**, *35*, 184–191.
8. Coelhoso, I.M.; Cardoso, M.M.; Viegas, R.M.C.; Crespo, J.P.S.G. Transport mechanism and modelling in liquid membrane contactors. Sep. Purif. Technol. **2000**, *19*, 183–197.
9. D'Elia, N.A.; Dahuron, L.; Cussler, E.L. Liquid–liquid extractions with microporous hollow fibers. J. Mem. Sci. **1986**, *29*, 309–319.
10. Alonso, A.I.; Pantelides, C.C. Modelling and simulation of integrated membrane processes for recovery of Cr(VI) with Aliquat 336. J. Mem. Sci. **1996**, *110*, 151–167.
11. Peretti, S.W.; Tompkins, C.J.; Goodall, J.L.; Michaels, A.S. Extraction of 4-nitrophenol from 1-octanol into aqueous solution in a hollow fiber liquid contactor. J. Mem. Sci. **2001**, *195*, 193–202.
12. Viegas, R.M.C.; Rodriguez, M.; Luque, S.; Alvarez, J.R.; Coelhoso, I.M.; Crespo, J.P.S.G. Mass transfer correlations in membrane extraction: analysis of Wilson plot methodology. J. Mem. Sci. **1998**, *145*, 129–142.
13. Takeda, Y.; Yasui, A.; Morita, M.; Katsuta, S. Extraction of sodium and potassium perchlorates with benzo-18-crown-6 into various organic solvents. Quantitative elucidation of anion effects on the extraction-ability and -selectivity for $Na^+$ and $K^+$. Talanta, **2002**, *56*, 505–513.

14. Pierre, F.X.; Souchon, I.; Marin, M. Recovery of sulfur aroma compounds using membrane-based solvent extraction. J. Mem. Sci. **2001**, *187*, 239–253.
15. Mc Dowell, W.J.; Case, G.N.; Aldrup, D.W. Investigation of ion - size - selective Synergism in solvent extraction. Separ. Sci. Technol. **1983**, *18* (14&15), 1483–1507.
16. Cussler, E.L. *Diffusion Mass Transfer in Fluid Systems*, 2nd Ed.; Cambridge University press, 1997.
17. Marcus, Y.; Asher, L.E. Extraction of alkali halides from their aqueous solutions by crown ethers. J. Phys. Chem. **1978**, *82*, 1246–1254.
18. Bondi, A. *Physical Properties of Molecular Crystals, Liquids and Glasses*, Wiley: New York, 1968.
19. Pierre, F.X.; Souchon, I.; Athes, V.; Marin, M. Extraction liquide–liquide à membrane de composés d'aromes soufrés: influence des conditions hydrodynamiques dans un module de fibres creuses. Récents Progrès en Génie des Procédés, **2001**, *15* (81), 307–314.
20. Juang, R.S.; Huang, H.L. Mechanistic analysis of solvent extraction of heavy metals in membrane contactors. J. Mem. Sci. **2003**, *213*, 125–135.
21. Behr, J.P.; Kirch, M.; Lehn, J.M. Carrier-mediated transport though bulk liquid membranes: dependence of transport rates and selectivity on carrier properties in a diffusion-limited process. J. Am. Chem. Soc. **1985**, *107*, 241–246.
22. Madsen, N.K.; Sincovec, R.F. PDECOL: general collocation software for partial differential equations. ACM Trans. Math. Software, **1979**, *3*, 326–351.
23. Gawronski, R.; Wrzesinska, B. Kinetics of solvent extraction in hollow fiber contactors. J. Mem. Sci. **2000**, *168*, 213–222.
24. Lipnizki, F.; Field, R.W. Mass transfer performance for hollow fibre modules with shell side axial feed flow: using an engineering approach to develop a framework. J. Mem. Sci. **2001**, *193*, 195–208.
25. Viegas, R.M.C.; Rodriguez, M.; Luque, S.; Alvarez, J.R.; Coelhoso, I.M.; Crespo, J.P.S.G. Mass transfer correlations in membrane extraction: analysis of Wilson-plot methodology. J. Mem. Sci. **1998**, *145*, 129–142.
26. Prasad, R.; Sirkar, K.K. Dispersion-free solvent extraction with micro-porous hollow-fiber modules **1988**, *34* (2), 177–188.

Received February 1, 2004
Accepted September 14, 2004